ACS Chemical Neuroscience

Research Article

pubs.acs.org/chemneuro

Discovery of Lacosamide Affinity Bait Agents That Exhibit Potent Voltage-Gated Sodium Channel Blocking Properties

Ki Duk Park,[‖,#,▽] Xiao-Fang Yang,[†,#] Hyosung Lee,[‖,#] Erik T. Dustrude,[§,#] Yuying Wang,[†,○] Rajesh Khanna,*[,†,‡,§] and Harold Kohn*[,⊥,‖]

[†]Departments of Pharmacology and Toxicology, [‡]Biochemistry and Molecular Biology, and [§]Program in Medical Neuroscience, Paul and Carole Stark Neurosciences Research Institute, Indiana University School of Medicine, Indianapolis, Indiana 46202, United States

[‖]Division of Chemical Biology and Medicinal Chemistry, UNC Eshelman School of Pharmacy, and [⊥]Department of Chemistry, University of North Carolina, Chapel Hill, North Carolina 27599, United States

ABSTRACT: Lacosamide ((*R*)-**1**) is a recently marketed, first-in-class, antiepileptic drug. Patch-clamp electrophysiology studies are consistent with the notion that (*R*)-**1** modulates voltage-gated Na^+ channel function by increasing and stabilizing the slow inactivation state without affecting fast inactivation. The molecular pathway(s) that regulate slow inactivation are poorly understood. Affinity baits are chemical reactive units, which when appended to a ligand (drug) can lead to irreversible, covalent modification of the receptor thus permitting drug binding site identification including, possibly, the site of ligand function. We describe, herein, the synthesis of four (*R*)-**1** affinity baits, (*R*)-*N*-(4″-isothiocyanatobiphenyl-4′-yl)methyl 2-acetamido-3-methoxypropionamide ((*R*)-**8**), (*S*)-*N*-(4″-isothiocyanatobiphenyl-4′-yl)methyl 2-acetamido-3-methoxypropionamide ((*S*)-**8**), (*R*)-*N*-(3″-isothiocyanatobiphenyl-4′-yl)methyl 2-acetamido-3-methoxypropionamide ((*R*)-**9**), and (*R*)-*N*-(3″-acrylamidobiphenyl-4′-yl)methyl 2-acetamido-3-methoxypropionamide ((*R*)-**10**). The affinity bait compounds were designed to interact with the receptor(s) responsible for (*R*)-**1**-mediated slow inactivation. We show that (*R*)-**8** and (*R*)-**9** are potent inhibitors of Na^+ channel function and function by a pathway similar to that observed for (*R*)-**1**. We further demonstrate that (*R*)-**8** function is stereospecific. The calculated IC_{50} values determined for Na^+ channel slow inactivation for (*R*)-**1**, (*R*)-**8**, and (*R*)-**9** were 85.1, 0.1, and 0.2 μM, respectively. Incubating (*R*)-**9** with the neuronal-like CAD cells led to appreciable levels of Na^+ channel slow inactivation after cellular wash, and the level of slow inactivation only modestly decreased with further incubation and washing. Collectively, these findings have identified a promising structural template to investigate the voltage-gated Na^+ channel slow inactivation process.

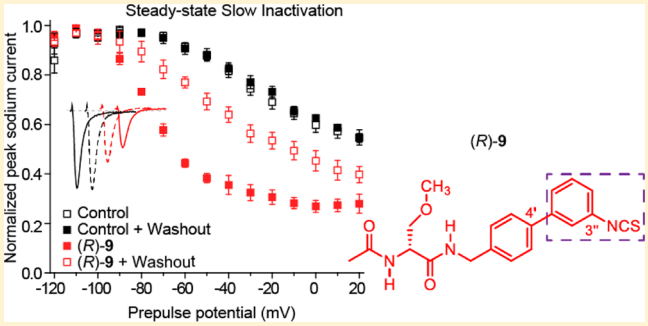

KEYWORDS: *Anti-epileptic, lacosamide, affinity bait agent, irreversible modification, voltage-gated sodium channel, slow inactivation*

Lacosamide[1] ((*R*)-**1**) is a first-in-class antiepileptic drug (AED) that has been marketed for adjuvant treatment of partial-onset seizures in adults.[2] Whole animal pharmacological studies showed that the (*R*)-**1** anticonvulsant profile is unique and prevents seizure spread by mechanisms different from other AEDs.[3] Radioligand displacement assays using more than 100 potential receptors did not reveal high-affinity binding targets.[4] These findings suggested that (*R*)-**1** function is unique or that binding is weak or both. Recent patch-clamp electrophysiology studies demonstrated that (*R*)-**1** modulated voltage-gated Na^+ channel (VGSC) function by likely increasing and stabilizing the slow inactivation process without affecting fast inactivation.[5−8] The experimental findings were also consistent with a mechanism in which (*R*)-**1** blocks fast inactivated channels with very slow kinetics.[5,6] No other anticonvulsant is reported to preferentially modulate Na^+ channel slow inactivation. The molecular pathway for this interaction has not been determined; thus, it is not known whether (*R*)-**1** exerts its activity by directly interacting with the Na^+ channel or through an intermediary protein.

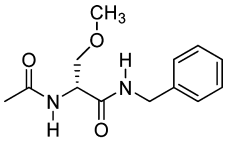

(*R*)-**1**

Affinity baits are chemical reactive units that lead to irreversible, covalent modification of the receptor when they are appended to a ligand (drug) (Figure 1, **2** + **3** ⇌ **4** → **5**).[9−21] This technology has been used to identify binding

Received: October 25, 2012
Accepted: December 29, 2012
Published: December 29, 2012

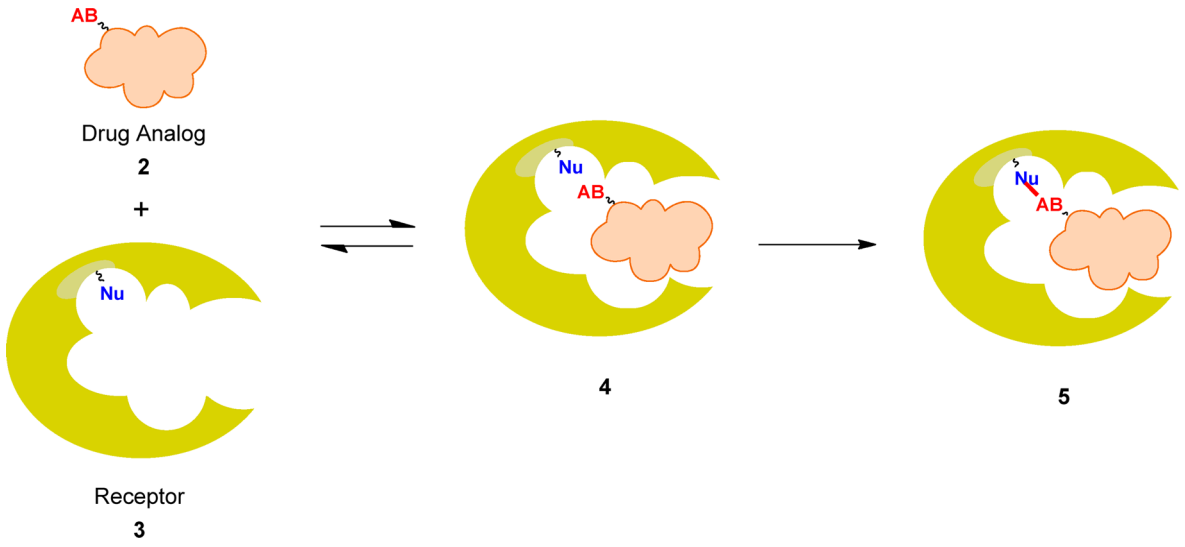

Figure 1. Affinity bait (AB) and strategy for target receptor modification. Proposed pathway for receptor modification by a ligand that binds with modest affinity to its cognate receptor. Ligand **2** reversibly binds to receptor **3** to provide complex **4**. Modification of the receptor by **2** proceeds through the affinity bait (AB) to give covalent ligand−receptor adduct **5**.

partners and their approximate binding location when ligand binding is modest. Different electrophilic and photoactivable affinity bait units have been advanced.[9−14] Among the electrophilic affinity baits are isothiocyanate and acrylamide groups.[14−16,20−30] Isothiocyanates and acrylamides display an excellent balance between stability and reactivity; they do not readily react with hydroxylic solvents (thus permitting their dissolution in aqueous solutions) but do react with biological nucleophiles (e.g., thiols, amines) with minimal nonspecific background labeling of cellular constituents.[9,28−30]

We have shown that the lacosamide 4′-isothiocyanate affinity bait agent (*R*)-**6** given orally to rats exhibited anticonvulsant activity comparable to (*R*)-**1** in the maximal electroshock seizure (MES) test[31] (ED_{50} (mg/kg): (*R*)-**1**, 3.9; (*R*)-**6**, 4.2).[32] We also demonstrated that (*R*)-**6**, like (*R*)-**1**, likely promoted Na^+ channel slow inactivation in catecholamine A differentiated (CAD) cells (IC_{50} (μM): (*R*)-**1**, 85; (*R*)-**6**, 8.1).[7] Finally, we found that (*R*)-**6** increased this Na^+ channel inactivation far more effectively than (*S*)-**6** (IC_{50} (μM): (*R*)-**6**, 8.1; (*S*)-**6**, 68), a finding consistent with their activities in the MES test in rats (ED_{50} (mg/kg): (*R*)-**6**, 4.2; (*S*)-**6**, >180).[32] When we incubated (*R*)-**6** (five times the calculated slow inactivation IC_{50} value) with CAD cells (37 °C, 10 min), it retained only a modest increase (∼10%) in the levels of inactivation after (*R*)-**6** was removed from the reaction solution (cellular wash), indicating a low efficiency of covalent adduction by the affinity bait reagent.[7] Recently, we reported that the *N*-(biphenyl-4′-yl)methyl amide derivative (*R*)-**7**,[33] which differed from (*R*)-**1** by an incorporated 4′-aryl unit (see box in (*R*)-**7**), had greater Na^+ channel inactivation in CAD cells than (*R*)-**1** (calculated slow inactivation IC_{50} (μM): (*R*)-**1**, 85; (*R*)-**7**, 2.9).[34] This finding suggested that lacosamide-like affinity bait compounds containing a *N*-(biphenyl-4′-yl)methyl amide unit would lead to a comparable increase in slow inactivation, and with CAD cell incubation an increased percentage of the Na^+ channels irreversibly converted to the slow-inactivated state.

Here we report the synthesis of a series of (*R*)-**1** affinity bait agents ((*R*)-**8**−(*R*)-**10**) designed to interact with the receptor(s) responsible for (*R*)-**1**-mediated slow inactivation. We show that the isothiocyanate analogues (*R*)-**8** and (*R*)-**9**

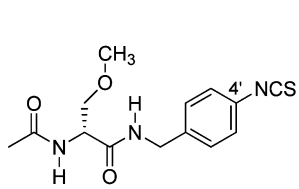

(*R*)-**6**

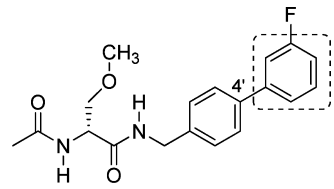

(*R*)-**7**

potently modulated Na^+ channel inactivation similar to (*R*)-**1** and that (*R*)-**8** function was stereospecific. We further show that (*R*)-**9** incubation with CAD cells led to appreciable levels of inactivated Na^+ channels consistent with slow inactivation after cellular wash and that the extent of slow inactivation only modestly decreased with further heating and cellular wash. The implications of these findings are discussed.

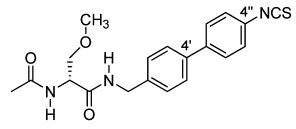

(*R*)-**8**

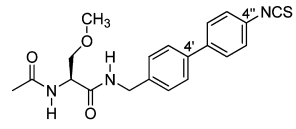

(*S*)-**8**

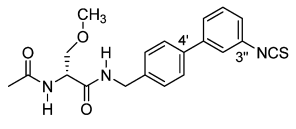

(*R*)-**9**

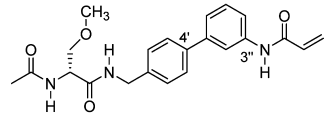

(*R*)-**10**

RESULTS

Chemistry. Affinity bait agents (*R*)-**8**, (*S*)-**8**, (*R*)-**9**, and (*R*)-**10** were prepared using a similar route to the one used to construct 4′-substituted (*R*)-**1** analogues[35] (Scheme 1). Optically pure 2-acetamido-3-methoxypropionic acid[35] (**16**) was coupled through its mixed anhydride[36] with either (4″-*N*-(*tert*-butoxycarbonyl)aminobiphenyl-4′-yl)methylamine (**14**) or (3″-*N*-(*tert*-butoxycarbonyl)aminobiphenyl-4′-yl)methylamine (**15**) without racemization to give **17** and **18**. Amines **14** and **15** were prepared by Suzuki coupling[37] ($Pd(PPh_3)_4$, K_2CO_3) of

dx.doi.org/10.1021/cn300188h | *ACS Chem. Neurosci.* 2013, 4, 463−474

Scheme 1. Synthesis of Affinity Compounds

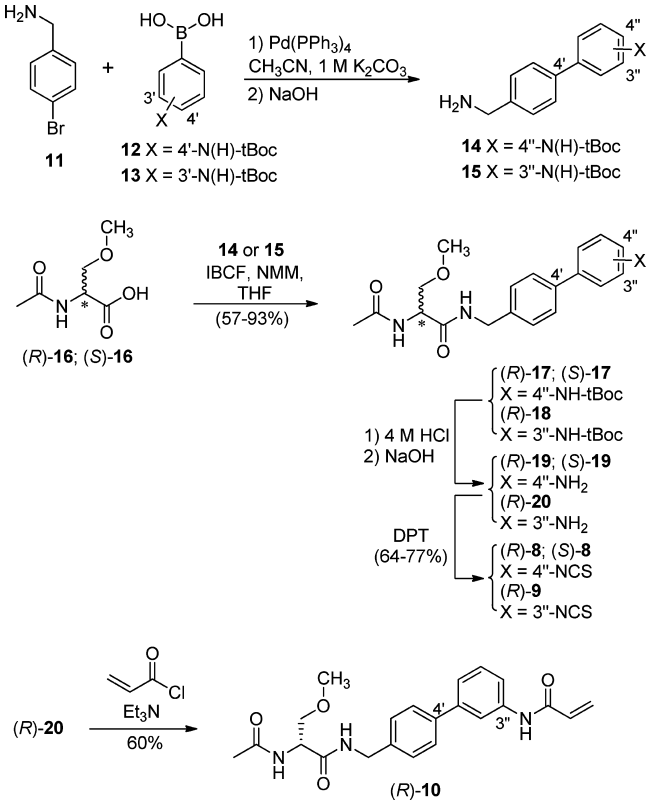

4-bromobenzylamine (**11**) and either 4-(**12**) or 3-(**13**) (*N*-*tert*-butoxycarbonylamino)phenylboronic acid. HCl deprotection of **17** and **18** gave the corresponding arylamines **19** and **20**, respectively, after basification, which was converted to the affinity bait agents (*R*)-**8**, (*S*)-**8**, and (*R*)-**9** using di(2-pyridyl) thionocarbonate (DPT). Reaction of (*R*)-**20** with acryloyl chloride and triethylamine gave acrylamide (*R*)-**10**. We confirmed the optical purity of (*R*)-**8**, (*S*)-**8**, (*R*)-**9**, and (*R*)-**10** by ^{1}H NMR using the chiral resolving agent (*R*)-(−)-mandelic acid.[38]

Pharmacology. *Inhibition of Na$^+$ Currents by (R)-8, (S)-8, (R)-9, and (R)-10.* Using the whole-cell patch-clamp configuration, we examined the effects of the affinity bait compounds on voltage-gated Na$^+$ channels in CAD cells. We previously reported that CAD cells express endogenous tetrodotoxin-sensitive Na$^+$ currents with rapid activation and inactivation kinetics upon membrane depolarization and are likely composed of Na$^+$ channel isoforms $Na_V1.7$, $Na_V1.1$, and $Na_V1.3$.[7,39,40] Our results have demonstrated that the Na$^+$ channel properties of (*R*)-**1** in CAD cells[7] were similar to those reported in neurons in culture and in mouse N1E-115 neuroblastoma cells.[5] Accordingly, we used readily accessible CAD cells to evaluate the effects of the affinity bait compounds on Na$^+$ channel function, recognizing in advance that CAD cells do not express the same set of Na$^+$ channels expressed in CNS neurons. First, we tested the ability of the affinity bait agents to inhibit peak inward Na$^+$ currents by holding CAD cells at −80 mV and executing a current (*I*)−voltage (*V*) protocol, which consisted of 15-ms-step depolarizations ranging from −70 to +80 mV (in +10 mV increments; Figure 2A). An exemplar trace of the peak currents from untreated cells and those treated with 1 μM of (*R*)-**8** and (*R*)-**9** are illustrated in Figure 2B. Compared to control currents (peak current value of

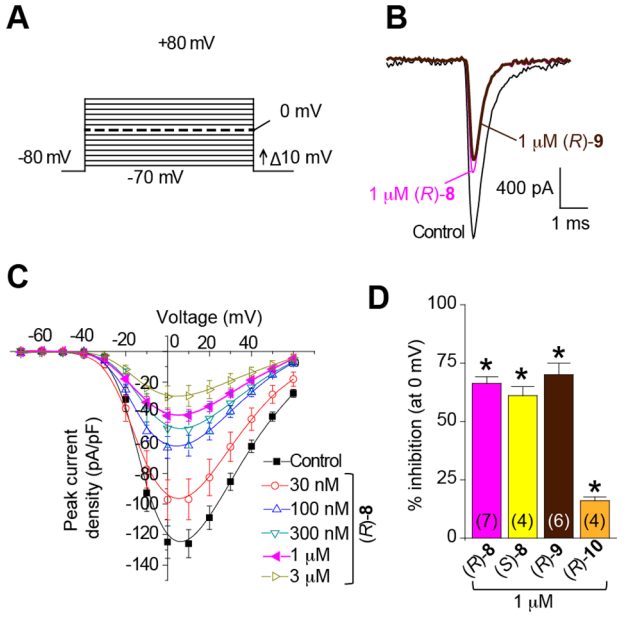

Figure 2. Inhibition of macroscopic Na$^+$ currents by affinity bait derivatives of lacosamide. (A) Voltage protocol used to elicit macroscopic Na$^+$ currents in CAD cells. (B) Representative current responses, at a step voltage to 0 mV, of CAD treated with 0.1% DMSO control, 1 μM (*R*)-**8**, and 1 μM (*R*)-**9**. (C) Summary of peak current−voltage (*I*−*V*) relationships for CAD cells treated with 0.1% DMSO (control) or varying concentrations of (*R*)-**8** (n = 4−8). Current responses were evoked by a step from a holding potential of −80 mV and stepping up in 10 mV increments from −70 to +60 mV. (D) Percent inhibition of peak current density (pA/pF), at 0 mV, from CAD cells treated with 1 μM of (*R*)-**8**, (*S*)-**8**, (*R*)-**9**, and (*R*)-**10.** Inhibition was determined by normalizing peak currents in each drug condition to average peak currents obtained in DMSO-treated cells. Asterisks indicate statistically significant differences in peak inhibition between predrug (control) and the indicated concentrations of (*R*)- and (*S*)-compounds (p < 0. 05, ANOVA with posthoc Dunnett's test). Numbers in parentheses are the number of cells patched per condition.

−124.9 ± 10.5 pA/pF at +0 mV for untreated cells (n = 9)), peak macroscopic Na$^+$ currents were inhibited by 60−70% for (*R*)-**8**, (*S*)-**8**, and (*R*)-**9** and ∼16% for (*R*)-**10** (Figure 2). The inhibition of Na$^+$ currents was not accompanied by changes in reversal potential for any of the affinity bait compounds (data not shown).

As changes in current inhibition could be due to changes in channel gating properties, we tested if the affinity bait compounds altered the voltage-dependence of activation of Na$^+$ currents in CAD cells. Changes in activation for the CAD cells treated with the affinity bait compounds were measured by whole-cell ionic conductances by comparing their respective midpoints ($V_{1/2}$) and slope factors (k) in response to changes in command voltage (Figure 3, right curves). The calculated $V_{1/2}$ and k values (Table 1) showed that activation $V_{1/2}$ was shifted by 3.1 and 5.9 mV in the depolarizing direction by (*R*)-**8** and (*S*)-**8**, respectively, and by 7.9 and 1.7 mV in the hyperpolarizing direction by (*R*)-**9** and (*R*)-**10**, respecively. There were no appreciable shifts in slope values compared to control except for a slight increase in slope with 100 nM of (*R*)-**9**. Thus, these results suggest that (*R*)-**8**, (*S*)-**8**, and (*R*)-**9**, but not (*R*)-**10**, are effective inhibitors of peak Na$^+$ currents, and that maximal inhibition is observed for affinity bait compounds possessing the (*R*)-configuration.

dx.doi.org/10.1021/cn300188h | ACS Chem. Neurosci. 2013, 4, 463−474

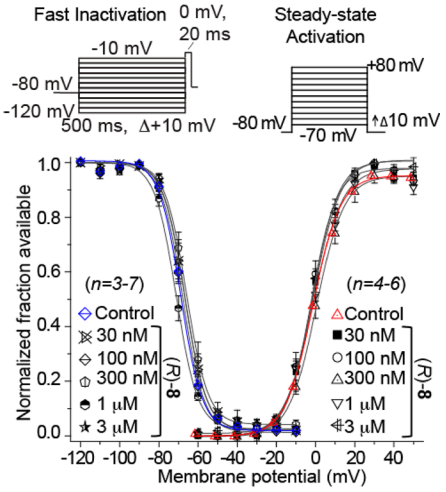

Figure 3. Effects of isothiocyanate compound (*R*)-**8** on activation and inactivation properties of Na^+ currents in CAD cells. Values for $V_{1/2}$, the voltage of half-maximal activation and steady-state fast inactivation and the slope factors (k) were derived from Boltzmann distribution fits to the individual recordings and averaged to determine the mean (±SEM) voltage dependence of activation and fast inactivation. The voltage protocol used to evoke current responses for each protocol is shown above the fits. Representative Boltzmann fits for activation and steady-state inactivation for CAD cells treated with 0.1% DMSO (control) and indicated concentrations of (*R*)-**8** are shown. The calculated values for $V_{1/2}$ and k of activation and steady-state inactivation for all concentrations of the four affinity bait compounds tested in this study are presented in Tables 1 and 2, respectively.

*Fast Inactivation Properties of Na^+ Currents in CAD Cells Are Not Affected by (R)-**8**, (S)-**8**, (R)-**9**, and (R)-**10**.* Since our data were consistent that most of the lacosamide-like affinity bait agents exhibited profound effects on Na^+ channels slow-inactivated state (see Figures 4−7), we determined if these compounds could alter steady-state fast inactivation using a previously described protocol designed to induce a fast-inactivated state.[7,39] Cells were held at −80 mV, stepped to inactivating prepulse potentials ranging from −120 to −10 mV (in 10 mV increments) for 500 ms, then the cells were stepped to 0 mV for 20 ms to measure the available current (Figure 3, top left protocol). A 500 ms conditioning pulse was used because it allowed all of the endogenous channels to transition to a fast-inactivated state at all potentials examined. Steady-state, fast inactivation curves of Na^+ currents from DMSO-, (*R*)-**8**-, (*S*)-**8**-, (*R*)-**9**-, and (*R*)-**10**-treated CAD cells were well fitted with a single Boltzmann function (R^2 > 0.967 for all conditions). The Boltzmann curves for (*R*)-**8**-treated cells are illustrated in Figure 3 (leftmost curves). The $V_{1/2}$ value for inactivation for 0.1% DMSO-treated cells was −68.4 ± 3.1 mV (n = 9), which was not significantly different from the $V_{1/2}$ values of most concentrations of (*R*)-**8**-, (*S*)-**8**-, (*R*)-**9**-, or (*R*)-**10**- treated cells (Table 2; p > 0.05; ANOVA with a posthoc Dunnett's test). The 100 nM concentration of (*R*)-**9** caused a significant hyperpolarizing shift of ∼14 mV (Table 1) with no commensurate change in slope compared to control cells. The slopes of fast inactivation were not affected by the affinity bait agents. Similar results were observed for (*R*)-**1** and (*R*)-**6**.[7]

*(R)-**8**, (S)-**8**, (R)-**9**, and (R)-**10** Affect the Transition to a Slow-Inactivated State of Na^+ Currents in CAD Cells.* Recent studies indicate that (*R*)-**1** reduces VGSC availability by selectively increasing VGSCs' transition to a slow-inactivated state.[5−8,39] We recognize that the observed data is also consistent with a mechanism where (*R*)-**1** blocks Na^+ fast inactivated channels with very slow kinetics.[41] Like earlier researchers, we have assumed that (*R*)-**1**-induced Na^+ channel modulation proceeds by the slow inactivation pathway. Accordingly, we used protocols similar to those employed for (*R*)-**1**[5−8] and tested the ability of the affinity bait agents to modulate transition to the slow-inactivated state in CAD cells. CAD cells were held at −80 mV and conditioned to potentials ranging from −120 to +20 mV (in +10 mV increments) for 5 s. Then, fast-inactivated channels were allowed to recover for 150 ms at a hyperpolarized pulse to −120 mV, and the fraction of channels available was tested by a single depolarizing pulse, to 0 mV, for 15 ms (Figure 4A). This brief hyperpolarization allowed the channels to recover from fast inactivation while limiting recovery from slow inactivation.

A representative family of slow inactivation traces from CAD cells treated with 1 μM (*R*)-**9** is shown in Figure 4B. For comparison, representative current traces at −50 mV are highlighted. As reported earlier,[7,39] this potential was selected for three reasons: (1) most channels are undergoing steady-state inactivation, likely involving contributions from slow- and fast-inactivating pathways[42,43] where −50 mV is in the steep voltage-dependence range for each; (2) it approximates the resting membrane potential and approaches the action potential firing threshold of CNS neurons,[44] where slow inactivation appears to be physiologically important during sustained subthreshold depolarizations;[45] and (3) changes in the Na^+ channel availability near −50 mV can impact the window

Table 1. Comparative Boltzmann Parameters of Voltage-Dependence of Channel Activation Curves for the Respective Affinity Bait Reagents[a]

condition	concentration	$V_{1/2}$	k
control		−12.8 ± 0.5 (4)	7.4 ± 0.5 (4)
(*R*)-**8**	30 nM	−12.3 ± 0.8 (5)	6.6 ± 0.7 (5)
	100 nM	−12.9 ± 0.3 (5)	6.7 ± 0.3 (5)
	300 nM	−9.7 ± 0.7 (4)	7.3 ± 0.6 (4)
	1 μM	−11.3 ± 0.5 (5)	7.5 ± 0.4 (5)
	3 μM	−12.2 ± 0.5 (6)	7.1 ± 0.5 (6)
(*S*)-**8**	300 nM	−10.8 ± 0.4 (4)	6.9 ± 0.4 (4)
	1 μM	−6.9 ± 0.4 (5)*	7.1 ± 0.3 (5)
	3 μM	−9.1 ± 0.6 (5)	6.4 ± 0.5 (5)
	10 μM	−9.3 ± 0.4 (4)	7.1 ± 0.3 (4)
	30 μM	−13.7 ± 0.6 (5)	6.8 ± 0.5 (5)
(*R*)-**9**	300 pM	−16.9 ± 1.0 (4)	6.2 ± 0.7 (4)
	1 nM	−20.8 ± 2.0 (4)*	8.4 ± 1.5 (4)
	100 nM	−12.6 ± 1.8 (4)	10.0 ± 1.3 (4)
	1 μM	−15.0 ± 0.6 (2)	6.2 ± 0.6 (2)
(*R*)-**10**	3 μM	−13.0 ± 0.5 (4)	6.8 ± 0.4 (4)
	30 μM	−14.5 ± 1.0 (5)	6.3 ± 0.5 (5)
	100 μM	−13.9 ± 1.4 (5)	6.8 ± 1.1 (5)
	300 μM	−13.8 ± 1.7 (4)	6.9 ± 1.0 (4)

[a]Values for $V_{1/2}$, the half-maximal activation, and the slope factors (k) were derived from Boltzmann distribution fits to the individual recordings and averaged to determine the mean and standard error (± SEM) displayed above. Asterisk (*) indicates statistical significance (p < 0.05) compared to control values (one-way ANOVA with Tukey's posthoc test).

dx.doi.org/10.1021/cn300188h | ACS Chem. Neurosci. 2013, 4, 463−474

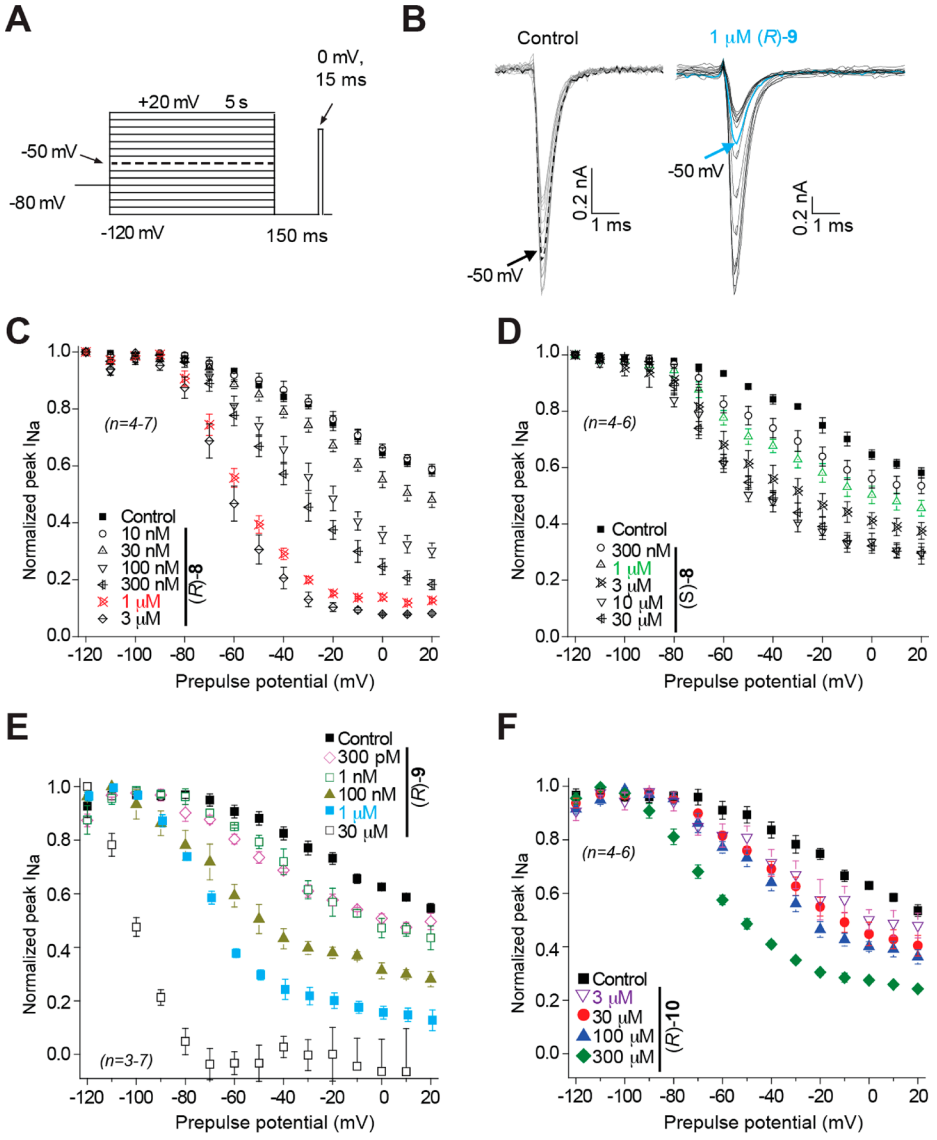

Figure 4. Affinity bait compounds affect steady-state slow inactivation state of Na^+ currents in CAD cells. (A) Voltage protocol utilized to isolate the slow inactivated fraction of currents. Currents were evoked by 5 s prepulses between −120 and −20 mV, and then fast-inactivated channels were allowed to recover for 150 ms at a hyperpolarized pulse to −120 mV. The fraction of channels available at 0 mV was then analyzed. (B) Representative family of current traces from CAD cells in the presence of DMSO (control) or 1 μM (*R*)-**9**. The dashed black (control) and solid blue traces ((*R*)-**9**) in the current recordings depict the current at −50 mV (also highlighted by dashes in the voltage protocol). (C−F) Summary of steady-state, slow-activation curves for CAD cells treated with (*R*)-**8** (C), (*S*)-**8** (D), (*R*)-**9** (E), and (*R*)-**10** (F). Drug-induced slow inactivation was more prominent in CAD cells treated with (*R*)-**8** and (*R*)-**9** than (*S*)-**8** or (*R*)-**10** at almost all concentrations tested.

current of Na^+ current activation and inactivation under steady-state conditions.[43,46] Compared with control (untreated cells), adding (*R*)-**8** to CAD cells induced a greater decrease in the fraction of current available than (*S*)-**8**. When we added 1 μM (*R*)-**8** to CAD cells, we found that, at −50 mV, 0.39 ± 0.01 fractional units (n = 5) of the Na^+ current were available compared with DMSO-treated cells after a 10 min incubation period, suggesting that in these cells a large fraction (0.61 ± 0.01; calculated as 1 minus the normalized I_{Na}) of the channels transitioned to a nonconducting (slow-inactivated) state (Figure 4C). Correspondingly, in the 30 μM (*S*)-**8**-treated cells, the slow-inactivated fraction was 0.29 ± 0.05 (Figure 4D). A similar enantioselective increase of slow inactivation was observed for **1** and **6**.[7] When we treated CAD cells with either (*R*)-**9** (1 μM) or (*R*)-**10** (1 μM), substantial levels of slow inactivation were observed at −50 mV for only (*R*)-**9** (fraction of the channels to transition to a nonconducting (slow-inactivated) state: (*R*)-**9**, 0.62 ± 0.03 (n = 4); (*R*)-**10**, 0.20 ± 0.04 (n = 5)) (Figure 4E, F).

To further understand the extent to which the four affinity bait compounds induced slow inactivation, we determined the concentration response curves for slow inactivation induction for each compound (Figure 4C−F). Using the Boltzmann equation, we fit the voltage dependence of slow inactivation for the control and for each of the drug concentrations. This yielded a $V_{1/2}$ value of slow inactivation for each concentration, which was then plotted against the concentration used. Finally, fits of the concentration response of slow inactivation against the $V_{1/2}$ of slow inactivation provided an IC_{50} value. This value is likely a reflection of presumptive drug binding and bonding to a slow inactivation site on the Na^+ channels. Compared with our recently reported IC_{50} values of 85 and 8.1 μM for slow

dx.doi.org/10.1021/cn300188h | ACS Chem. Neurosci. 2013, 4, 463−474

Table 2. Comparative Boltzmann Parameters of Voltage-Dependence of Channel Steady-State Fast Inactivation Curves for the Respective Affinity Bait Reagents[a]

condition	concentration	$V_{1/2}$	k
control		−68.4 ± 3.1 (5)	4.6 ± 1.6 (5)
(*R*)-**8**	30 nM	−66.5 ± 1.2 (5)	4.4 ± 0.4 (5)
	100 nM	−67.6 ± 2.1 (5)	4.9 ± 0.3 (5)
	300 nM	−66.6 ± 0.8 (5)	5.4 ± 0.5 (4)
	1 μM	−70.8 ± 1.2 (5)	5.0 ± 0.3 (5)
	3 μM	−67.8 ± 0.6 (6)	5.1 ± 0.5 (6)
(*S*)-**8**	300 nM	−68.8 ± 0.3 (4)	4.9 ± 0.3 (4)
	1 μM	−64.2 ± 0.3 (5)	4.8 ± 0.3 (5)
	3 μM	−65.0 ± 0.3 (5)	4.9 ± 0.2 (5)
	10 μM	−73.0 ± 0.5 (4)	5.7 ± 0.4 (4)
	30 μM	−70.7 ± 0.3 (5)	5.1 ± 0.3 (5)
(*R*)-**9**	300 pM	−78.6 ± 1.3 (4)*	5.4 ± 0.6 (4)
	1 nM	−76.8 ± 1.3 (4)	5.1 ± 0.6 (4)
	100 nM	−82.4 ± 2.3 (4)*	6.9 ± 0.9 (4)
	1 μM	−75.9 ± 2.9 (3)	4.2 ± 0.9 (3)
(*R*)-**10**	3 μM	−70.4 ± 0.7 (5)	6.1 ± 0.7 (5)
	30 μM	−69.6 ± 0.7 (5)	4.2 ± 0.6 (5)
	100 μM	−69.7 ± 4.2 (5)	3.1 ± 4.2 (5)
	300 μM	−73.7 ± 1.0 (4)	5.5 ± 0.6 (4)

[a]Values for $V_{1/2}$, the half-maximal fast inactivation, and the slope factors (k) were derived from Boltzmann distribution fits to the individual recordings and averaged to determine the mean and standard error (± SEM) displayed above. Asterisk (*) indicates statistical significance ($p < 0.05$) compared to control values (one-way ANOVA with Tukey's posthoc test).

inactivation by (*R*)-**1** and (*R*)-**6**, respectively,[7] the IC_{50} values for the (*R*)-**8**, (*S*)-**8**, (*R*)-**9**, and (*R*)-**10** were 100.1 nM ± 3.8 (R^2 = 0.988), 1.1 ± 0.2 μM (R^2 = 0.994), 202.8 nM ± 8.9 (R^2 = 0.979), and 401.0 ± 9.8 μM (R^2 = 0.987), respectively. The enantioselective effect observed for **8** (IC_{50} (*S*)-**8**/IC_{50} (*R*)-**8**: 11.0) mirrored that found for **6** (IC_{50} (*S*)-**6**/IC_{50} (*R*)-**6**: 8.4).[7]

These data are consistent with the notion that (*R*)-**8** and (*R*)-**9** effectively increased the transition of Na^+ channels to a slow-inactivated state. We showed that for **8** this activity preferentially resided in the (*R*)-stereoisomer. Moreover, we demonstrated that adding the aryl group to (*R*)-**6** to give (*R*)-**8** led to an ∼80-fold decrease (increased potency) in the CAD cell IC_{50} value for slow inactivation induction. Similarly, for (*R*)-**9**, a positional isomer of (*R*)-**8**, we observed a ∼40-fold decrease in the IC_{50} value versus (*R*)-**6**.

Extent of Slow Inactivation by (R)-8 and (R)-9 due to Covalent Modification. The enhanced potency of (*R*)-**8** and (*R*)-**9** compared with (*R*)-**6** in increasing slow inactivation may represent the combined effects of the affinity bait agent binding to the receptor(s) (Figure 1, **4**) and the subsequent covalent adduction of the affinity bait agent (Figure 1, **5**). Thus, we asked if the observed increase in slow inactivation was due, in part, to the formation of stable, covalent adduct(s). If the affinity bait agent irreversibly affects Na^+ channel slow inactivation by covalently modifying a receptor, then slow inactivation may still be observed when the drug derivative is removed from the CAD cells by extensive washing with an extracellular bath solution. Alternatively, if the affinity bait agent increases Na^+ channel slow inactivation by a reversible process, then when the agent is removed from the test reaction recovery from slow inactivation should be observed.

To distinguish between these possibilities, we treated CAD cells with either (*R*)-**1**, (*R*)-**8**, or (*R*)-**9** at five times their calculated slow inactivation IC_{50} values for 10 min, which is expected to inhibit >99% of the slow inactivation, extensively washed the cells (three times) over a 10 min period, and then the level of slow inactivation was determined (Figure 5A). We found that the extent of Na^+ channel slow inactivation for the CAD cells treated with either (*R*)-**1** or (*R*)-**8** after washing was nearly the same as that of untreated cells, while cells treated with (*R*)-**9** and then washed still retained 19% of the Na^+ channels in the slow inactivated state (Figure 5B). The comparable levels of slow inactivation for the (*R*)-**1**-treated, (*R*)-**8**-treated, and untreated cells after cellular wash indicated that the wash conditions were sufficient to remove the affinity bait agents from the test solution and resulted in no loss of channel function. The level of Na^+ channel slow inactivation for

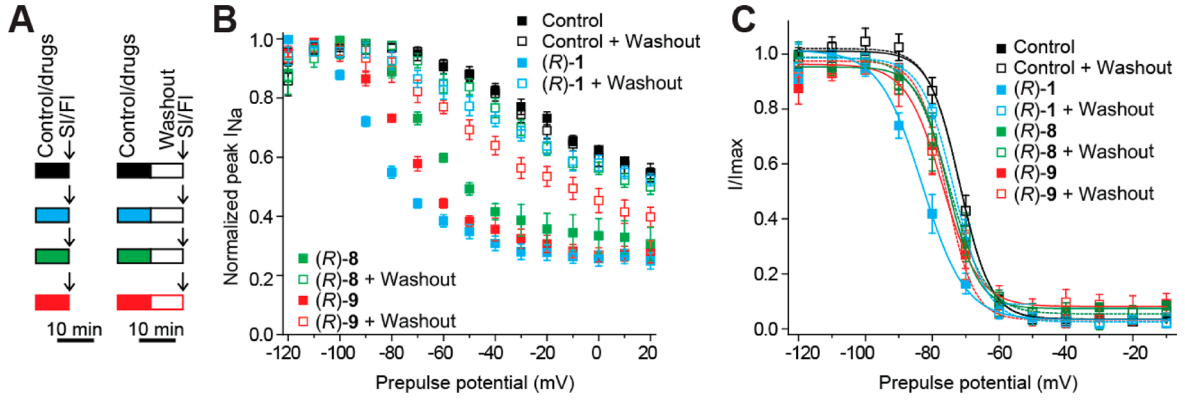

Figure 5. Effect of (*R*)-**8** and (*R*)-**9** on Na^+ currents slow inactivation (SI) and fast inactivation (FI). (A) Experimental design for the washout experiments. For this and subsequent figures, the experiments were conducted on separate sets of cells in parallel with SI and FI assessments performed at the times indicated by the arrows. Drugs were not applied under voltage clamp. (B) Summary of steady-state, slow inactivation curves for CAD cells treated with 0.1% DMSO (control) or lacosamide ((*R*)-**1**) and affinity bait reagents at concentrations representing 5-fold the calculated IC_{50} values for slow inactivation (i.e., 425 μM for (*R*)-**1**, 0.5 μM (*R*)-**8**, and 1 μM (*R*)-**9**). Curves with open symbols represent SI following a 10 min wash. (C) Representative Boltzmann fits for fast inactivation for CAD cells treated with 0.1% DMSO (control) and various concentrations of the indicated compounds before and after wash conditions are shown. Data are from 4–8 cells per condition.

dx.doi.org/10.1021/cn300188h | ACS Chem. Neurosci. 2013, 4, 463–474

(*R*)-**9** was approximately two times higher than reported for (*R*)-**6** after cellular wash,[7] indicating that (*R*)-**9** was a more effective affinity bait agent. Additionally, we measured fast inactivation in these conditions and observed that $V_{1/2}$ and k values of (*R*)-**8** or (*R*)-**9** were not significantly different from those of control-treated cells (Figure 5C).

Next, we asked if the level of Na^+ channel slow inactivation is retained under the experimental test conditions (37 °C) for extended times, since isothiocyanate covalent adduction has been shown to be reversible in some cases.[45−47] CAD cells were treated with 1 μM (*R*)-**9** (five times the slow inactivation IC_{50} value) at 37 °C (10 min), the level of slow inactivation determined by patch-clamp electrophysiology, the cells washed (three times, total 10 min), heated at 37 °C an additional 15 or 60 min, washed a second time (three times, total 10 min), and then the level of slow inactivation measured (Figure 6A). We observed the extent of slow inactivation (−50 mV) changed from 19% to 16% after 15 min of incubation (37 °C) and cellular wash, and to 12% after additional 60 min incubation and cellular wash (Figure 6B, bars i, ii), indicating that the modified receptor(s) generated by putative (*R*)-**9** adduction is likely to be sufficiently stable to permit further characterization (e.g., receptor site identification). Again, we measured fast inactivation in these conditions and observed that $V_{1/2}$ and k values were not changed by the incubation or wash conditions employed (Figure 6C).

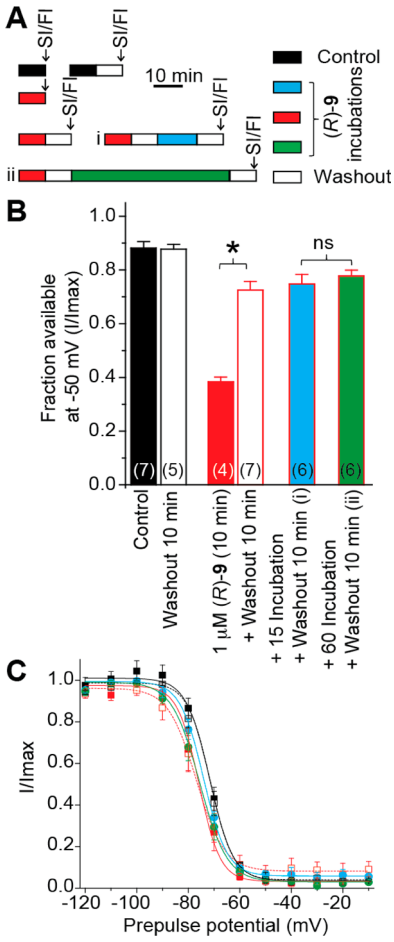

Figure 6. Effect of the (*R*)-**9** covalent modified adduct on slow inactivation as a function of time. (A) Experimental design for the varying incubation and washout conditions. (B) Summary of the fraction of current available at −50 mV for CAD cells treated with 0.1% DMSO (control) or 1 μM (*R*)-**9** without and with wash and varying incubations (as indicated in (A)). Asterisk (∗) indicates statistically significant differences in fraction of current available between the 1 μM (*R*)-**9** condition and following washout of 1 μM (*R*)-**9** ($p < 0.05$, one-way ANOVA with Dunnett's posthoc test). (C) Representative Boltzmann fits for fast inactivation for CAD cells treated with 0.1% DMSO (control) and various concentrations of the indicated compounds before and after wash conditions are shown. Numbers in parentheses are the number of cells patched per condition.

Extent of (R)-9-Mediated Na^+ Channel Slow Inactivation Increases with (R)-9 Incubation Time. To support the finding that (*R*)-**9** incubation with CAD cells led to covalent adduction (Figure 1, **4** → **5**) and an increased level of cells in the slow-inactivated state, we treated CAD cells with 1 μM (five times the slow inactivation IC_{50} value) for different time periods (3, 10, 30 min) at 37 °C, determined the fraction of cells in the presumed slow-inactivated state, then washed the CAD cells (three times, total: 10 min), and then again determined the fraction of cells in the slow-inactivated state (Figure 7A). We expected that those Na^+ channels *irreversibly* converted to the slow-inactivated state would increase with incubation time provided sufficient amounts of (*R*)-**9** remained in the cell. We found that the amount of Na^+ channel slow inactivation after cellular wash progressively increased to 23% over the 30 min time course (Figure 7B, open bars). Correspondingly, we observed little change in the extent of fast inactivation over this time course versus the control (drug untreated) samples after cellular wash (Figure 7C). Interestingly, the fraction of Na^+ channels that transitioned to the slow-inactivated state prior to cellular wash reached 62% after the first 10 min, but then diminished to 45% after 30 min (Figure 7B, solid bars). We have tentatively attributed this trend to the consumption of (*R*)-**9** by cellular constituents (e.g., glutathione) and the buffer prior to reacting with the receptor(s) responsible for Na^+ channel slow inactivation. If this is the case, the reduced (*R*)-**9** cellular concentration will decrease the levels of Na^+ channels in the slow-inactivated state that result from noncovalent binding of (*R*)-**9** to the receptor(s) (Figure 1, **4**). Collectively, these results indicate that (*R*)-**9** covalently modifies a receptor(s) mediating Na^+ channel slow inactivation and that the adduct is sufficiently stable under the test conditions.

DISCUSSION

We designed the lacosamide-like affinity bait agents (*R*)-**6**, (*R*)-**8**, (*R*)-**9**, and (*R*)-**10** to potently inactivate the Na^+ channel slow inactivation process by covalent modification (Figure 1). Successful adduction requires that the affinity bait agent efficiently binds to the receptor(s) in close proximity to a nucleophilic residue on the receptor(s) (Figure 1, **2** + **3** ⇌ **4**), and that the geometry for adduction of the affinity bait by the nucleophile is correct (Figure 1, **4** → **5**). Compounds (*R*)-**6**, (*R*)-**8**, and (*R*)-**9** contained an isothiocyanate affinity bait. In (*R*)-**6**, the isothiocyanate moiety was placed in the 4′-position of the *N*-benzyl amide moiety. In (*R*)-**8** and (*R*)-**9**, the isothiocyanate group was placed at the 4″ and 3″ positions of the *N*-(biphenyl-4′-yl)methyl amide group, respectively. Finally, in (*R*)-**10**, we positioned an acrylamide affinity moiety at the 3″ position of the *N*-(biphenyl-4′-yl)methyl amide group. We found that adding an aryl unit in the *N*-benzyl amide moiety of (*R*)-**6** to give (*R*)-**8** and (*R*)-**9** markedly enhanced Na^+ current inhibition (Figure 2). Like the cases of **1** and its 4′-isothiocyanate derivative **6**,[7] **8**-mediated Na^+ channel inactivation preferentially occurred with the (*R*)-stereoisomer

dx.doi.org/10.1021/cn300188h | ACS Chem. Neurosci. 2013, 4, 463−474

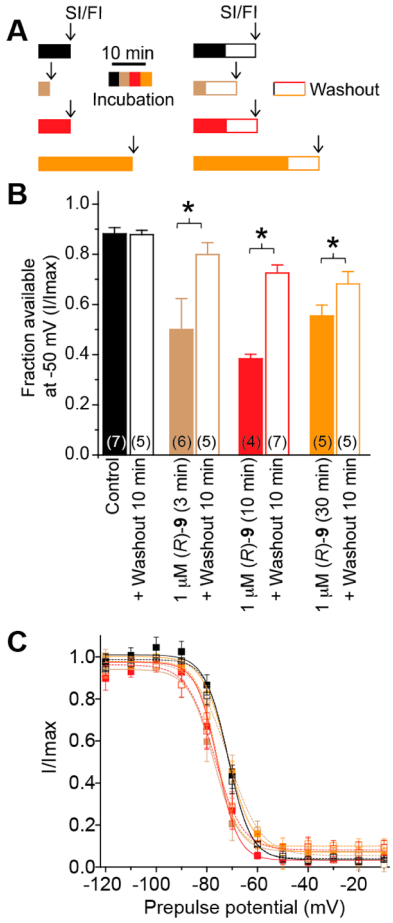

Figure 7. Effect of reaction times on (*R*)-**9** mediated steady-state slow inactivation state of Na^+ currents in CAD cells. (A) Experimental design for the varying incubation and washout conditions. (B) Summary of the fraction of current available at −50 mV for CAD cells treated with 0.1% DMSO (control) or treated with 1 μM (*R*)-**9** for 3, 10, and 30 min (closed bars) and following washout of each of these conditions (open bars). Asterisks (∗) indicate statistically significant differences in fraction of current available between the 1 μM (*R*)-**9** condition and following its corresponding washout condition or compared to control at the 10 min incubation time ($p < 0.05$, one-way ANOVA with Dunnett's posthoc test). (C) Representative Boltzmann fits for fast inactivation for CAD cells treated with 0.1% DMSO (control) and various concentrations of the indicated compounds before and after wash conditions are shown. Data are from 4−7 cells per condition.

compared with the (*S*)-isomer (Figures 2 and 4). We further demonstrated that (*R*)-**8** and (*R*)-**9**, like (*R*)-**1**, preferentially increased Na^+ channel slow inactivation but not fast inactivation processes (Figure 4, Table 2). Addition of the aryl unit to (*R*)-**6** to give (*R*)-**8** led to an ∼80-fold increase in Na^+ channel slow inactivation activity. Similarly, we observed an ∼40-fold increase in slow inactivation activity in going from (*R*)-**6** to (*R*)-**9** (IC_{50} (μM): (*R*)-**6**, 8.1;[7] (*R*)-**8**, 0.1; (*R*)-**9**, 0.2). The decreases in the IC_{50} values for (*R*)-**8** and (*R*)-**9** compared with (*R*)-**6** are similar to the decrease reported in proceeding from (*R*)-**1** to (*R*)-**7** (IC_{50} (μM): (*R*)-**1**, 85;[7] (*R*)-**7**, 2.9[34]). Substitution of the 3″-isothiocyanate moiety in (*R*)-**9** by the 3″-acrylamide unit to give (*R*)-**10** led to a sharp increase in the IC_{50} value for Na^+ channel slow inactivation, suggesting that the increase in steric size that accompanies this structural change affected binding (IC_{50} (μM): (*R*)-**9**, 0.2; (*R*)-**10**, 401.0) (Figure 4). Additional studies will be needed to confirm if the size of the 3″-substituent affects binding (Figure 1, **2** + **3** ⇌ **4**). Together, these findings indicated that aryl extension of the (*R*)-**1** framework, in select cases, did not principally alter the mode of function of these agents but did increase their ability to modulate the Na^+ channel slow inactivation process.

Compounds (*R*)-**8** and (*R*)-**9** were designed to act as affinity bait reagents, wherein the isothiocyanate group was incorporated to react with a nearby nucleophilic residue on the receptor(s) upon compound binding. Since isothiocyanate-based affinity baits have been shown, in some cases, to undergo reversible covalent modification,[47−49] we tested whether the CAD cell Na^+ channels remained in the slow inactivation state after (*R*)-**8** or (*R*)-**9** treatment and cellular wash, and whether slow inactivation was observed upon further heating. We found that using concentrations that were five times the affinity bait agents' IC_{50} value, that (*R*)-**9**, but not (*R*)-**8**, led to increased levels of slow inactivation after cellular wash (Figure 5), and that with further heating the level of slow inactivation for the treated (*R*)-**9** CAD cells remained nearly constant for the first 15 min and then modestly decreased after 60 min of heating (Figure 6B). To further support the notion that the incubation of CAD cells with (*R*)-**9** led to the covalent modification of a receptor(s) responsible for slow inactivation, we showed that lengthening the incubation times from 3 to 30 min increased the level of Na^+ channel slow inactivation after cellular wash (Figure 7B). The nonreversible modification of Na^+ channels by (*R*)-**9** could have two functional effects on channel kinetics: (*R*)-**9**-bound channels remain closed or (*R*)-**9**-bound channels promote an inactive state, but the channels are still able to cycle through closed, open, and inactive states. In the first case, bound channels should have no contribution to available current and, consequently, there should be no shift in the slow inactivation availability curve following a channel inactivating protocol. Our data (Figure 5B) shows that, following incubation with (*R*)-**9** and subsequent washout, a 5 s inactivating pulse reduces the available current compared to control. These results support the second scenario, in which (*R*)-**9**-bound Na^+ channels are available to contribute current in response to depolarized conditioning pulses that promote resting, closed state. In the case of depolarized conditioning pulses that promote inactivation, the available current is reduced, suggesting that (*R*)-**9**-bound channels have enhanced transition into, or inhibit exit from, an inactivated conformation.

The findings that Na^+ channel slow inactivation but not fast inactivation properties in CAD cells were likely affected with (*R*)-**9** treatment (Figure 4, Table 2) and that these effects remained after cellular wash are important (Figure 5). Previous studies have shown that reversible agents, such as (*R*)-**1**, affected only slow inactivation.[5−7] Our findings now show that (*R*)-**9** can retain a fraction of the channels in a slow inactivated state refractory to washout. Moreover, our findings support previous projections that fast and slow inactivation are uncoupled.[50]

CONCLUSIONS

We have discovered a promising structural template to investigate the voltage-gated Na^+ channel slow inactivation process. The molecular pathway (or pathways) that promote slow inactivation are poorly understood and several domains in the Na^+ channel have been implicated in the conformational change needed to affect current flow.[46,51,52] We anticipate that

dx.doi.org/10.1021/cn300188h | ACS Chem. Neurosci. 2013, 4, 463−474

(*R*)-**9** or similar agents may prove useful to identify the receptor(s) and the structural site on the receptor responsible for Na^+ channel slow inactivation. This information is expected to be useful in future drug design efforts.

METHODS

Chemistry. *(4″-N-(tert-Butoxycarbonyl)aminobiphenyl-4′-yl)-methylamine (**14**).* To a dry CH_3CN solution (15 mL) of *p*-bromobenzylamine (**11**) (0.78 g, 4.2 mM) was added 4-(*N*-*tert*-butoxycarbonylamino)phenylboronic acid (**12**) (1.00 g, 4.2 mM). Then, a solution of 1 N K_2CO_3 (15 mL) was added and the mixture was stirred and heated at reflux under Ar. After 15 min, tetrakis-(triphenylphosphine)palladium(0) (0.19 g, 0.2 mM) was added and stirred at 90 °C (12−16 h). The mixture was filtered and evaporated in vacuo. The resulting residue was dissolved in EtOAc (100 mL) and washed with H_2O (100 mL) and brine (100 mL). The organic layer was dried (Na_2SO_4). Concentrated aqueous HCl (0.1 mL) was added to the organic layer and stirred at room temperature (1 h), and the precipitate filtered and washed with hexanes to obtain (4″-*N*-(*tert*-butoxycarbonyl)aminobiphenyl-4′-yl)methylamine hydrochloride as a yellow solid (0.88 g, 62%): R_f = 0.00 (hexanes/EtOAc 1/2); mp 242−244 °C; ^{1}H NMR (DMSO-d_6) δ 1.49 (s, C(C**H**$_3$)$_3$), 4.03−4.04 (br m, C**H**$_2$), 7.56−7.68 (m, 8 Ar**H**), 8.59 (s, N**H**$_3$Cl), 9.47 (s, N**H**); ^{13}C NMR (DMSO-d_6) δ 28.1 (C(**C**H$_3$)$_3$), 41.8 (**C**H$_2$), 79.1 (**C**(CH$_3$)$_3$), 118.4, 126.1, 126.8, 129.5, 132.6, 133.0, 139.3, 139.8 (Ar**C**), 155.2 (N**C**(O)O); HRMS (ESI$^+$) 321.1630 [M − HCl + Na]$^+$ (calcd for $C_{18}H_{22}N_2O_2Na^+$ 321.1620).

The resulting solid was added to a NaOH solution (pH 10, 100 mL), and then the aqueous layer extracted with CH_2Cl_2 (3 × 100 mL). The organic layers were combined, dried (Na_2SO_4), and concentrated in vacuo. The resulting residue (0.72 g, 92%) was used without further purification.

*(R)-N-(4″-N-(tert-Butoxycarbonyl)aminobiphenyl-4′-yl)methyl 2-Acetamido-3-methoxypropionamide ((R)-**17**).* To a cooled THF solution (−78 °C, dry ice acetone bath) of (*R*)-**16**[29] (0.18 g, 1.1 mmol) were successively added *N*-methylmorpholine (NMM) (0.18 mL, 1.6 mmol), stirred for 2 min, isobutylchloroformate (IBCF) (0.18 mL, 1.4 mmol), stirred for 5 min, and then **14** (0.39 g, 1.3 mmol). Upon addition, the reaction mixture was allowed to warm to room temperature and further stirred (2−3 h). The salts were filtered and rinsed with THF, and the filtrate was concentrated in vacuo. The residue obtained was purified by column chromatography on SiO_2 to give (*R*)-**17** as a white solid (0.34 g, 70%): R_f = 0.45 (MeOH/$CHCl_3$ 1/15); mp 187−188 °C; $[\alpha]^{26}_D$ −12.7° (*c* 1.1, $CHCl_3$); ^{1}H NMR ($CDCl_3$) δ 1.53 (s, C(C**H**$_3$)$_3$), 2.04 (s, C(O)C**H**$_3$), 3.40 (s, OC**H**$_3$), 3.45 (dd, *J* = 7.6, 9.2 Hz, CH**H**′OCH$_3$), 3.82 (dd, *J* = 4.0, 9.2 Hz, CH**H**′OCH$_3$), 4.45−4.58 (m, C**H**$_2$N, C**H**), 6.44 (d, *J* = 6.4 Hz, N**H**CH), 6.55 (s, N**H**-*t*Boc), 6.76−6.79 (br t, N**H**CH$_2$), 7.23 (d, *J* = 8.6 Hz, 2 Ar**H**), 7.42 (d, *J* = 8.6 Hz, 2 Ar**H**), 7.49−7.53 (m, 4 Ar**H**); ^{13}C NMR (DMSO-d_6) δ 22.5 (C(O)**C**H$_3$), 28.1 (C(**C**H$_3$)$_3$), 41.7 (N**C**H$_2$), 52.6 (O**C**H$_3$), 58.2 (OCH$_2$**C**H), 72.1 (O**C**H$_2$CH), 79.1 (**C**(CH$_3$)$_3$), 118.4, 125.9, 126.7, 127.5, 133.5, 137.9, 138.2, 138.9 (Ar**C**), 152.7 (N**C**(O)O), 169.5, 169.8 (2 **C**(O)); HRMS (ESI$^+$) 574.1320 [M + Cs]$^+$ (calcd for $C_{24}H_{31}N_3O_5Cs^+$ 574.1318).

*(S)-N-(4″-N-(tert-Butoxycarbonyl)aminobiphenyl-4′-yl)methyl 2-Acetamido-3-methoxypropionamide ((S)-**17**).* Utilizing the preceding procedure and using (*S*)-**16** (0.13 g, 0.8 mmol), NMM (0.14 mL, 1.2 mmol), IBCF (0.14 mL, 1.0 mmol), and **14** (0.30 g, 1.0 mmol) gave (*S*)-**17** (0.24 g, 65%) as a white solid: R_f = 0.45 (MeOH/$CHCl_3$ 1/15); mp 186−188 °C; $[\alpha]^{26}_D$ +12.9° (*c* 1.0, $CHCl_3$); ^{1}H NMR (DMSO-d_6) δ 1.49 (s, C(C**H**$_3$)$_3$), 1.88 (s, C(O)C**H**$_3$), 3.27 (s, OC**H**$_3$), 3.48−3.55 (m, C**H**$_2$OCH$_3$), 4.31 (d, *J* = 6.0 Hz, C**H**$_2$N), 4.47−4.52 (m, C**H**), 7.29 (d, *J* = 8.0 Hz, 2 Ar**H**), 7.52−7.57 (m, 6 Ar**H**), 8.08 (d, *J* = 8.0 Hz, N**H**CH), 8.49 (t, *J* = 6.0 Hz, N**H**CH$_2$), 9.41 (s, N**H**-*t*Boc); ^{13}C NMR (DMSO-d_6) δ 22.5 (C(O)**C**H$_3$), 28.2 (C(**C**H$_3$)$_3$), 41.7 (N**C**H$_2$), 52.5 (O**C**H$_3$), 58.2 (OCH$_2$**C**H), 72.1 (O**C**H$_2$CH), 79.1 (**C**(CH$_3$)$_3$), 118.3, 125.9, 126.7, 127.5, 133.5, 137.9, 138.2, 138.9 (Ar**C**), 152.8 (N**C**(O)O), 169.5, 169.8 (2 **C**(O)); HRMS (ESI$^+$) 574.1268 [M + Cs]$^+$ (calcd for $C_{24}H_{31}N_3O_5Cs^+$ 574.1318).

*(R)-N-(4″-Isothiocyanatobiphenyl-4′-yl)methyl 2-Acetamido-3-methoxypropionamide ((R)-**8**).* (*R*)-**17** (0.26 g, 0.6 mmol) was dissolved in CH_2Cl_2 (5 mL) and treated with 4 M HCl in dioxane (0.7 mL) at room temperature (4 h). The resulting precipitate was filtered and washed with hexanes. The resulting solid was added to a NaOH solution (pH 10, 50 mL), and then the aqueous layer extracted with CH_2Cl_2 (3 × 50 mL). The organic layers were combined, dried (Na_2SO_4), and concentrated in vacuo. The resulting residue was dissolved in THF (10 mL) and treated with di(2-pyridyl) thionocarbonate (DPT) (0.24 mg, 1.0 mmol) at room temperature (16 h). The solvent was removed in vacuo, and the product was purified by silica gel column chromatography (1/9 acetone/EtOAc) to give 0.17 g (75%) of (*R*)-**8** as a white solid: R_f = 0.45 (acetone/EtOAc 1/9); mp 225−226 °C; $[\alpha]^{26}_D$ −20.2° (*c* 0.3, $CHCl_3$); IR (nujol) 3280, 2924, 2859, 2084, 1633, 1547, 1458, 1374, 1109, 926, 811 cm^{-1}; ^{1}H NMR (DMSO-d_6) δ 1.88 (s, C(O)C**H**$_3$), 3.27 (s, OC**H**$_3$), 3.48−3.56 (m, C**H**$_2$OCH$_3$), 4.33 (d, *J* = 6.0 Hz, C**H**$_2$N), 4.48−4.53 (m, C**H**), 7.35 (d, *J* = 8.0 Hz, 2 Ar**H**), 7.51 (d, *J* = 7.8 Hz, 2 Ar**H**), 7.64 (d, *J* = 8.0 Hz, 2 Ar**H**), 7.74 (d, *J* = 7.8 Hz, 2 Ar**H**), 8.10 (d, *J* = 7.6 Hz, N**H**CH), 8.52 (t, *J* = 6.0 Hz, N**H**CH$_2$), addition of excess (*R*)-(−)-mandelic acid to a $CDCl_3$ solution of (*R*)-**8** gave only one signal for the acetyl methyl and one signal for the ether methyl protons; ^{13}C NMR (DMSO-d_6) δ 22.5 (C(O)**C**H$_3$), 41.7 (N**C**H$_2$), 52.6 (O**C**H$_3$), 58.2 (OCH$_2$**C**H), 72.1 (O**C**H$_2$CH), 126.4, 126.5, 127.7, 127.8, 129.0 (Ar**C**), 133.6 (N**C**S), 137.0, 139.2, 139.3 (Ar**C**), 169.4, 169.8 (2 **C**(O)); LRMS (ESI$^+$) 406.1 [M + Na]$^+$ (calcd for $C_{20}H_{21}N_3O_3SNa^+$ 406.1); Anal. Calcd. for $C_{20}H_{21}N_3O_3S$: C, 62.64; H, 5.52; N, 10.96; S, 8.36. Found: C, 62.48; H, 5.46; N, 10.80; S, 8.17.

*(S)-N-(4″-Isothiocyanatobiphenyl-4′-yl)methyl 2-Acetamido-3-methoxypropionamide ((S)-**8**).* Utilizing the preceding procedure and using (*S*)-**17** (0.15 g, 0.3 mmol), 4 M HCl in dioxane (0.4 mL), and DPT (0.22 mg, 0.2 mmol) gave 0.09 g (69%) of (*S*)-**8** as a white solid: R_f = 0.45 (acetone/EtOAc 1/9); mp 224−226 °C; $[\alpha]^{26}_D$ +20.7° (*c* 0.3, $CHCl_3$); IR (nujol) 3282, 2924, 2858, 2084, 1636, 1547, 1458, 1374, 1107, 922, 812, 727 cm^{-1}; ^{1}H NMR (DMSO-d_6) δ 1.88 (s, C(O)C**H**$_3$), 3.27 (s, OC**H**$_3$), 3.47−3.56 (m, C**H**$_2$OCH$_3$), 4.33 (d, *J* = 6.0 Hz, C**H**$_2$N), 4.47−4.52 (m, C**H**), 7.34 (d, *J* = 8.0 Hz, 2 Ar**H**), 7.51 (d, *J* = 8.4 Hz, 2 Ar**H**), 7.64 (d, *J* = 8.0 Hz, 2 Ar**H**), 7.74 (d, *J* = 8.4 Hz, 2 Ar**H**), 8.09 (d, *J* = 8.0 Hz, N**H**CH), 8.51 (t, *J* = 6.0 Hz, N**H**CH$_2$), addition of excess (*R*)-(−)-mandelic acid to a $CDCl_3$ solution of (*S*)-**8** gave only one signal for the acetyl methyl and one signal for the ether methyl protons; ^{13}C NMR (DMSO-d_6) δ 22.6 (C(O)**C**H$_3$), 41.7 (N**C**H$_2$), 52.7 (O**C**H$_3$), 58.2 (OCH$_2$**C**H), 72.1 (O**C**H$_2$CH), 126.4, 126.5, 127.7, 127.8, 129.0 (Ar**C**), 133.6 (N**C**S), 137.0, 139.2, 139.4 (Ar**C**), 169.4, 169.8 (2 **C**(O)); HRMS (ESI$^+$) 406.1203 [M + Na]$^+$ (calcd for $C_{20}H_{21}N_3O_3SNa^+$ 406.1201).

(3′-N-tert-Butoxycarbonylamino-biphenyl-4-yl)methylamine Hydrochloride. Employing the procedure described for **14** and using **11** (0.78 g, 4.2 mmol), acetonitrile (15 mL), **13** (1.00 g, 4.2 mmol), tetrakis(triphenylphosphine)palladium(0) (0.19 g 0.2 mmol), and aqueous 1 N K_2CO_3 (15 mL) gave the desired product (0.25 g, 35%) as a yellow solid: R_f = 0.00 (hexanes/EtOAc 1/1); mp 192−195 °C; ^{1}H NMR (CD_3OD) δ 1.53 (s, C(C**H**$_3$)$_3$), 4.14−4.18 (br s, C**H**$_2$N), 7.21−7.76 (m, 8 Ar**H**); ^{13}C NMR (DMSO-d_6) δ 28.6 (C(**C**H$_3$)$_3$), 42.3 (CH$_2$NH$_3$), 79.6 (**C**(CH$_3$)$_3$), 120.9, 127.1, 129.7, 130.0, 131.6, 131.8, 133.9, 140.5, 140.6, 140.8, (10 Ar**C**), 153.3 (HN**C**(O)); LRMS (ES$^+$) 299.18 [M − Cl]$^+$ (calcd for $C_{18}H_{23}N_2O_2^+$ 299.18); HRMS (ESI$^+$) 299.1755 [M − Cl]$^+$ (calcd for $C_{18}H_{23}N_2O_2^+$ 299.1754).

*(R)-N-(3″-tert-Butoxycarbonylaminobiphenyl-4′-yl)methyl 2-Acetamido-3-methoxypropionamide ((R)-**18**).* To an aqueous NaOH solution (pH = 10.0, 50 mL) was added the (3′-*tert*-butoxycarbonylaminobiphenyl-4-yl)methylamine hydrochloride (0.54 g, 1.6 mmol) and extracted with CH_2Cl_2 (3 × 50 mL). The organic layers were combined, dried (Na_2SO_4), and concentrated in vacuo. The resulting residue was further dried under high vacuum (16 h) to give the desired product (3′-*tert*-butoxycarbonylaminobiphenyl-4-yl)methylamine (**15**). The amine was immediately used without further purification.

Employing the procedure described for (*R*)-**8** and using (*R*)-**16** (0.26 g, 1.6 mmol), NMM (0.24 g, 2.4 mmol), IBCF (0.33 g, 2.4

dx.doi.org/10.1021/cn300188h | ACS Chem. Neurosci. 2013, 4, 463−474

mmol), and **15** gave the desired product (*R*)-**18** (405 mg, 57%) as a white solid: R_f = 0.36 (EtOAc/hexanes 1/1); mp 189−192 °C; $[\alpha]^{25}_D$ −12.9° (c 1.0, $CHCl_3$); ^{1}H NMR ($CDCl_3$) δ 1.53 (s, C(CH_3)$_3$), 2.02 (s, CH_3C(O)), 3.38 (s, OCH_3), 3.43−3.47 (m, CH*H*′OCH$_3$), 3.77−3.84 (m, CH*H*′OCH$_3$), 4.45−4.51 (d, *J* = 6.0 Hz, CH_2N), 4.55−4.61 (m, C*H*), 6.50−6.58 (br d, N*H*CH), 6.66 (s, N*H*C(O)O), 6.85−6.96 (br t, N*H*CH$_2$), 7.20−7.36 (m, 5 Ar*H*), 7.53 (d, *J* = 8.0 Hz, 2 Ar*H*), 7.62 (s, Ar*H*), addition of excess (*R*)-(−)-mandelic acid to a $CDCl_3$ solution of the product gave only one signal for the acetyl methyl and one signal for the ether methyl protons; ^{13}C NMR ($CDCl_3$) δ 23.3 (*C*H$_3$C(O)), 28.4 (C(*C*H$_3$)$_3$), 43.3 (N*C*H$_2$), 52.5 (*C*H), 59.2 (O*C*H$_3$), 71.8 (O*C*H$_2$), 80.7 (*C*(CH$_3$)$_3$), 117.3, 117.6, 121.8, 127.5, 127.9, 129.4, 137.1, 138.9, 140.2, 141.6 (10 Ar*C*), 152.9 (O*C*(O)NH), 170.1, 170.4 (*C*(O)); LRMS (ES$^+$) 442.19 [M + H]$^+$ (calcd for $C_{24}H_{32}N_3O_5^+$ 442.23); HRMS (ESI$^+$) 442.2336 [M + H]$^+$ (calcd for $C_{24}H_{32}N_3O_5^+$ 442.2341).

*(R)-N-(3″-Aminobiphenyl-4′-yl)methyl 2-Acetamido-3-methoxypropionamide ((R)-**20**).* To a solution of (*R*)-**18** (0.26 g, 0.59 mmol) in CH_2Cl_2 (5 mL) was added 4 M HCl in dioxane (0.7 mL) and stirred at room temperature (4 h). The reaction mixture was filtered and washed with hexanes. The resulting solid was added to an aqueous NaOH solution (pH 10, 50 mL) and the resulting mixture was extracted with CH_2Cl_2 (3 × 50 mL). The organic layers were combined, dried (Na_2SO_4), and concentrated in vacuo to give the desired product (*R*)-**20** (0.20 g, 100%) as a white solid: R_f = 0.21 (EtOAc); mp 99−100 °C; $[\alpha]^{23.5}_D$ +2.6 ° (c 0.25, $CHCl_3$); ^{1}H NMR ($CDCl_3$) δ 1.99 (s, C(O)CH_3), 3.36 (s, OCH_3), 3.45−3.56 (dd, *J* = 4.0, 9.2 Hz, CH*H*′OCH$_3$), 3.76−3.80 (dd, *J* = 7.2, 9.2 Hz, CH*H*′OCH$_3$), 4.41−4.46 (dd, *J* = 5.8, 15.0 Hz, CH*H*′N), 4.46−4.51 (dd, *J* = 5.8, 15.0 Hz, CH*H*′N), 4.59−4.64 (m, C*H*), 6.63−6.67 (m, N*H*CH, 1 Ar*H*), 6.85 (m, 1 Ar*H*), 6.93−6.96 (m, 1 Ar*H*), 6.99−7.05 (br t, N*H*CH$_2$), 7.20 (t, *J* = 7.8 Hz, 1 Ar*H*), 7.26 (d, *J* = 6.0 Hz, 2 Ar*H*), 7.49 (dd, *J* = 1.6, 6.4 Hz, 2 Ar*H*); ^{13}C NMR ($CDCl_3$/CD_3OD) δ 22.6 (C(O)*C*H$_3$), 43.2 (N*C*H$_2$), 53.0 (*C*H), 59.1 (O*C*H$_3$), 72.1 (O*C*H$_2$CH), 118.8, 123.0, 127.3, 127.4, 129.3, 137.1, 138.8, 140.0, 141.5 (9 Ar*C*), 170.4, 171.6 (2 *C*(O)), one aromatic resonance was not detected and is believed to overlap with nearby signals; LRMS (ES$^+$) 342.22 [M + H]$^+$ (calcd for $C_{19}H_{24}N_3O_3^+$ 342.17); HRMS (ESI$^+$) 342.1820 [M + H]$^+$ (calcd for $C_{19}H_{24}N_3O_3^+$ 342.1739).

*(R)-N-(3″-Isothiocyanatobiphenyl-4′-yl)methyl 2-Acetamido-3-methoxypropionamide ((R)-**9**).* To a solution of (*R*)-**20** (70 mg, 0.20 mmol) in dry THF (6 mL) was added DPT (96 mg, 0.41 mmol) and stirred at room temperature (16 h). The reaction mixture was concentrated in vacuo. The resulting residue was purified by silica gel column chromatography (acetone/EtOAc 1/9) to give the desired product (*R*)-**9** (0.17 g, 64%) as a white solid: R_f = 0.32 (EtOAc); mp 176−177 °C; $[\alpha]^{23.5}_D$ +1.0° (c 1.0, $CHCl_3$); ^{1}H NMR ($CDCl_3$) δ 2.02 (s, C(O)CH_3), 3.39 (s, OCH_3), 3.48 (dd, *J* = 7.2, 9.2 Hz, CH*H*′OCH$_3$), 3.81 (dd, *J* = 4.4, 9.2 Hz, CH*H*′OCH$_3$), 4.48−4.51 (m, CH_2N), 4.58−4.63 (m, C*H*), 6.59 (d, *J* = 6.8 Hz, N*H*CH), 7.03 (t, *J* = 5.4 Hz, N*H*CH$_2$), 7.18−7.20 (m, 1 Ar*H*), 7.32−7.50 (m, 7 Ar*H*), addition of excess (*R*)-(−)-mandelic acid to a $CDCl_3$ solution of the product gave only one signal for the acetyl methyl and one signal for the ether methyl protons; ^{13}C NMR ($CDCl_3$) δ 23.3 (C(O)*C*H$_3$), 43.3 (N*C*H$_2$), 52.8 (*C*H), 59.3 (O*C*H$_3$), 72.1 (O*C*H$_2$CH), 124.4, 124.6, 126.1, 127.5, 128.2, 130.2, 132.0 (7 Ar*C*), 135.9 (N*C*S), 138.1, 138.8, 142.6 (3 Ar*C*), 170.4, 170.7 (2 *C*(O)); LRMS (ES$^+$) 383.14 [M + H]$^+$ (calcd for $C_{20}H_{21}N_3O_3S^+$ 383.13); HRMS (ESI$^+$) 406.1199 [M + Na]$^+$ (calcd for $C_{20}H_{21}N_3O_3SNa^+$ 406.1201).

*(R)-N-(3″-Acrylamidobiphenyl-4′-yl)methyl 2-Acetamido-3-methoxypropionamide ((R)-**10**).* To a solution of (*R*)-**20** (100 mg, 0.29 mmol) in dry THF (6 mL) was added triethylamine (Et_3N) (45 mg 0.44 mmol) and acryloyl chloride (40 mg, 0.44 mmol) and stirred at room temperature (16 h). The reaction mixture was concentrated in vacuo. The resulting residue was purified by silica gel column chromatography (EtOAc) to give the desired product (*R*)-**10** (68 mg, 60%) as a white solid: R_f = 0.21 (CH_2Cl_2/MeOH 95/5); mp 183−184 °C; $[\alpha]^{23.5}_D$ +8.6°(c 0.1, $CHCl_3$/MeOH 95/5); ^{1}H NMR ($CDCl_3$/CD_3OD) δ 2.03 (s, C(O)CH_3), 3.37 (s, OCH_3), 3.52−3.56 (dd, *J* = 5.6, 9.6 Hz, CH*H*′OCH$_3$), 3.72 (dd, *J* = 4.6, 9.6 Hz, CH*H*′OCH$_3$), 4.40−4.50 (br s, CH_2N), 4.59 (dd, *J* = 4.6, 5.6 Hz, C*H*), 5.75 (dd, *J* = 2.4, 9.2 Hz, C(O)C*H*CH$_2$), 6.33−6.45 (m, C(O)CHCH_2), 7.30 (d, *J* = 8.0 Hz, 3 Ar*H*), 7.37 (t, *J* = 7.8 Hz, 1 Ar*H*), 7.54 (d, *J* = 8.4 Hz, 2 Ar*H*), 7.60 (d, *J* = 7.6 Hz, 1 Ar*H*), 7.87 (s, 1 Ar*H*), addition of excess (*R*)-(−)-mandelic acid to a $CDCl_3$/CD_3OD solution of the product gave only one signal for the acetyl methyl and one signal for the ether methyl protons; ^{13}C NMR ($CDCl_3$/CD_3OD) δ 22.6 (C(O)*C*H$_3$), 43.1 (N*C*H$_2$), 53.1 (*C*H), 59.0 (O*C*H$_3$), 72.1 (O*C*H$_2$CH), 118.8, 123.0, 127.3, 127.4 (4 Ar*C*), 127.8 (C(O)CH*C*H$_2$), 129.3 (Ar*C*), 131.3 (C(O)*C*HCH$_2$), 137.1, 138.8, 140.0, 141.5 (4 Ar*C*), 164.9, 170.5, 171.7 (3 *C*(O)), one downfield resonance was not detected and is believed to overlap with nearby signals; LRMS (ES$^+$) 418.25 [M + Na]$^+$ (calcd for $C_{22}H_{25}N_3O_4Na^+$ 418.17); HRMS (ESI$^+$) 418.1736 [M + Na]$^+$ (calcd for $C_{22}H_{25}N_3O_4Na^+$ 418.1743).

Catecholamine A Differentiated (CAD) Cells. CAD cells were grown at 37 °C and in 5% CO_2 (Sarstedt, Newton, NC) in Ham's F12/EMEM medium (GIBCO, Grand Island, NY), supplemented with 8% fetal bovine serum (FBS; Sigma, St. Louis, MO) and 1% penicillin/streptomycin (100% stocks, 10 000 U/mL penicillin G sodium and 10 000 μg/mL streptomycin sulfate).[7,34,39,40] Cells were passaged every 6−7 days at a 1:25 dilution. We typically observe variations in peak Na^+ current density, but not Na^+ channel isoform type (data not shown), over passages. Therefore, to minimize variation in current expression, all experiments for this paper were conducted with cells of a similar passage number.

Electrophysiology. Whole-cell voltage-clamp recordings were performed at room temperature on CAD cells using an EPC 10 amplifier (HEKA Electronics, Germany). Electrodes were pulled from thin-walled borosilicate glass capillaries (Warner Instruments, Hamden, CT) with a P-97 electrode puller (Sutter Instrument, Novato, CA) such that final electrode resistances were 1−2 MΩ when filled with internal solutions. The internal solution for recording Na^+ currents contained (in mM): 110 CsCl, 5 $MgSO_4$, 10 EGTA, 4 ATP Na_2-ATP, 25 Hepes (pH 7.2, 290−310 mOsm/L). The external solution contained (in mM) 100 NaCl, 10 tetraethylammonium chloride (TEA-Cl), 1 $CaCl_2$, 1 $CdCl_2$, 1 $MgCl_2$, 10 D-glucose, 4 4-AP, 0.1 $NiCl_2$, 10 Hepes (pH 7.3, 310−315 mOsm/L). Whole-cell capacitance and series resistance were compensated with the amplifier. Series resistance errors were compensated to be less than 3 mV by using 40−75% series resistance compensation and 1.0- to 2.0-MΩ pipettes. Linear leak currents were digitally subtracted by P/4. To negate any potential effects of time-dependent shifts in the voltage dependence of fast inactivation, we compared data obtained 3−4 min after establishing the whole-cell recording configuration from cells without drug against separate cells with the lacosamide derivatives.

Conditions for Incubation of Affinity Based Agents and Washes. These experiments were conducted on separate sets of cells in parallel. For experiments designed to determine if lacosamide derivatives interacted in a reversible or irreversible manner to affect slow inactivation, the agents (details of concentrations provided in the figure legends) were applied to the CAD cells for 10 min at 37 °C, then washed three times for a total of 10 min at 37 °C prior to whole-cell electrophysiology. The agents were not applied under voltage clamp. The washes (2 mL each) were performed using complete Ham's F12/EMEM medium. Cells were incubated at 37 °C during the washes. Following this washing regimen, the cells were placed in 0.5 mL of extracellular bathing solution for up to 3 min prior to establishing recording seals.

Data Acquisition and Analysis. Signals were filtered at 10 kHz and digitized at 10−20 kHz. Analysis was performed using Fitmaster and Origin8.1 (OriginLab Corporation, Northampton, MA). For activation curves, conductance (G) through Na^+ channels was calculated using the equation $G = I/(V_m - V_{rev})$, where V_{rev} is the reversal potential, V_m is the membrane potential at which the current was recorded, and I is the peak current. Activation and inactivation curves were fitted to a single-phase Boltzmann function $G/G_{max} = 1/\{1 + \exp[(V - V_{50})/k]\}$, where G is the peak conductance, G_{max} is the fitted maximal G, V_{50} is the half activation voltage, and k is the slope factor. Additional details of specific pulse protocols are described in the Results text or figure legends.

dx.doi.org/10.1021/cn300188h | ACS Chem. Neurosci. 2013, 4, 463−474

Statistical Analyses. Differences between means were compared by either paired or unpaired, two-tailed Student's *t*-tests or an analysis of variance (ANOVA), when comparing multiple groups (repeated measures whenever possible). If a significant difference is determined by ANOVA, then a Dunnett's or Tukey's posthoc test was performed. Data are expressed as mean ± SEM, with $p < 0.05$ considered as the level of significance.

AUTHOR INFORMATION

Corresponding Author

* E-mail addresses: khanna5@iu.edu (R.K.); harold_kohn@unc.edu (H.K.).

Present Addresses

[∇]K.D.P.: Center for Neuro-Medicine, Korea Institute of Science and Technology, Seoul, Korea.

[○]Y.W.: Department of Physiology and Pathophysiology, College of Medicine, Xi'an Jiaotong University, 76 Yanta West Road, Xi'an Province, 710061 Shaanxi, China.

Author Contributions

[#]These authors contributed equally to the work.

Author Contributions

K.D.P and H. L. synthesized the compounds. X.-F.Y., E.T.D., and Y.W. conducted whole cell electrophysiology. K.D.P., H.L., R.K., and H.K. designed this study, and R.K. and H.K. wrote the manuscript.

Funding

This work was supported by grants from the National Institutes of Health (R01NS054112 to H.K.), from the Indiana Clinical and Translational Sciences Institute funded, in part by a Project Development Team Grant Number (RR025761) from the National Institutes of Health, National Center for Research Resources, Clinical and Translational Sciences Award, the Indiana State Department of Health − Spinal Cord and Brain Injury Fund (A70-9-079138 to R.K.), a National Scientist Development from the American Heart Association (SDG5280023 to R.K.), and a Neurofibromatosis New Investigator Award from the Department of Defense Congressionally Directed Military Medical Research and Development Program (NF1000099 to R.K.).

Notes

The content is solely the responsibility of the authors and does not represent the official views of the National Center for Research Resources, National Institute of Neurological Disorders and Stroke, or the National Institutes of Health. H.K. has a royalty-stake position in (*R*)-**1**.

The authors declare no competing financial interest.

ABBREVIATIONS

AED, antiepileptic drug; VGSC, voltage-gated Na^+ channel; MES, maximal electroshock; CAD, catecholamine A differentiated; DPT, di(2-pyridyl) thionocarbonate; IBCF, isobutylchloroformate; $Na_v1.x$, voltage-gated Na^+ channel isoform 1.x; I_{Na}, Na^+ current; NMM, *N*-methylmorpholine

REFERENCES

(1) Choi, D., Stables, J. P., and Kohn, H. (1996) Synthesis and anticonvulsant activities of *N*-benzyl-2-acetamidopropionamide derivatives. *J. Med. Chem. 39*, 1907−1916.

(2) Perucca, E., Yasothan, U., Clincke, G., and Kirkpatrick, P. (2008) Lacosamide. *Nat. Rev. Drug Discovery 7*, 973−974.

(3) Stoehr, T., Kupferberg, H. J., Stables, J. P., Choi, D., Harris, R. H., Kohn, H., Walton, N., and White, H. S. (2007) Lacosamide, a novel anticonvulsant drug, shows efficacy with a wide safety margin in rodent models for epilepsy. *Epilepsy Res. 74*, 147−154.

(4) Beyreuther, B., Freitag, J., Heers, C., Krebsfaenger, N., Scharfenecker, U., and Stoehr, T. (2007) Lacosamide: a review of preclinical properties. *CNS Drug Rev. 13*, 21−42.

(5) Errington, A. C., Stohr, T., Heers, C., and Lees, G. (2008) The investigational anticonvulsant lacosamide selectively enhances slow inactivation of voltage-gated sodium channels. *Mol. Pharmacol. 73*, 157−169.

(6) Sheets, P. L., Heers, C., Stoehr, T., and Cummins, T. R. (2008) Differential block of sensory neuronal voltage-gated sodium channels by lacosamide, lidocaine and carbamazepine. *J. Pharmacol. Exp. Ther. 326*, 89−99.

(7) Wang, Y., Park, K. D., Salome, C., Wilson, S. M., Stables, J. P., Liu, R., Khanna, R., and Kohn, H. (2011) Development and characterization of novel derivatives of the antiepileptic drug lacosamide that exhibit far greater enhancement in slow inactivation of voltage-gated sodium channels. *ACS Chem. Neurosci. 2*, 90−106.

(8) Niespodziany, I., Leclere, N., Vandenplas, C., Foerch, P., and Wolff, C. Comparative study of lacosamide and classical sodium channel blocking antiepileptic drugs on sodium channel slow inactivation. *J. Neurosci. Res.* DOI: 10.1002/jnr.23136.

(9) Takemori, A. E., and Portoghese, P. S. (1985) Affinity labels for opioid receptors. *Annu. Rev. Pharmacol. Toxicol. 25*, 193−223.

(10) Drahl, C., Cravatt, B. F., and Sorensen, E. J. (2005) Protein-reactive natural products. *Angew. Chem. Intl. Ed. 44*, 5788−5809.

(11) Bayley, H., and Staros, J. V. (1984) In *Azides and Nitrenes: Reactivity and Utility*, Chapter 9, pp 433−490, Academic Press, Orlando, FL.

(12) Bucher, G. (2003) In *CRC Handbook of Organic Photochemistry and Photobiology* (Horspool, W., and Lenci, F., Eds.), 2nd ed., Chapter 44, pp 44-1−44-31, CRC Press, Boca Raton, FL.

(13) Speers, A. E., and Cravatt, B. F. (2004) Profiling enzyme activities in vivo using click chemistry methods. *Chem. Biol. 11*, 535−546.

(14) Park, K. D., Morieux, P., Salome, C., Cotten, S. W., Reamtong, O., Eyers, C., Gaskell, S. J., Stables, J. P., Liu, R., and Kohn, H. (2009) Lacosamide isothiocyanate-based agents: novel agents to target and identify lacosamide receptors. *J. Med. Chem. 52*, 6897−6911.

(15) Park, K. D., Stables, J. P., Liu, R., and Kohn, H. (2010) Proteomic searches comparing two (*R*)-lacosamide affinity baits: an electrophilic arylisothiocyanate and a photoactivated arylazide group. *Org. Biomol. Chem. 8*, 2803−2813.

(16) Park, K. D., Kim, D., Reamtong, O., Eyers, C., Gaskell, S. J., Liu, R., and Kohn, H. (2011) Identification of a lacosamide binding protein using an affinity bait and chemical reporter strategy: 14-3-3 ζ. *J. Am. Chem. Soc. 133*, 11320−11330.

(17) Staub, I., and Sieber, S. A. B. (2009) β-Lactam probes as selective chemical-proteomic tools for the identification and functional characterization of resistance associated enzymes in MRSA. *J. Am. Chem. Soc. 131*, 6271−6276.

(18) Hoffstrom, B. G., Kaplan, A., Letso, R., Schmid, R. S., Turmel, G. J., Lo, D. C., and Stockwell, B. R. (2010) Inhibitors of protein disulfide isomerase suppress apoptosis induced by misfolded proteins. *Nat. Chem. Biol. 6*, 900−906.

(19) Perez, D. I., Palomo, V., Perez, C., Gil, C., Dans, P. D., Luque, F. J., Conde, S., and Martinez, A. (2011) Switching reversibility to irreversibility in glycogen synthase kinase 3 inhibitors: clues for specific design of new compounds. *J. Med. Chem. 54*, 4042−4056.

(20) Paulick, M. G., and Bogyo, M. (2011) Development of activity-based probes for cathepsin X. *ACS Chem. Biol. 6*, 563−572.

(21) Tantama, M., Lin, W. C., and Licht, S. (2008) An activity-based protein profiling probe for the nicotinic acetylcholine receptor. *J. Am. Chem. Soc. 130*, 15766−15767.

(22) de Costa, B. R., Rothman, R. B., Bykov, V., Jacobson, A. E., and Rice, K. C. (1989) Selective and enantiospecific acylation of κ opioid receptors by (1*S*,2*S*)-*trans*-2-isothiocyanato-*N*-methyl-*N*-[2-(1-pyrrolidinyl)cyclohexyl]- benzeneacetamide. Demonstration of κ receptor heterogeneity. *J. Med. Chem. 32*, 281−283.

(23) de Costa, B. R., Lewin, A. H., Rice, K. C., Skolnick, P., and Schoenheimer, J. A. (1991) Novel site-directed affinity ligands for GABA-gated chloride channels: Synthesis, characterization, and molecular modeling of 1-(isothiocyanatophenyl)-4-*tert*-butyl-2,6,7-trioxabicyclo[2.2.2]octanes. *J. Med. Chem. 34*, 1531−1538.
(24) Rice, K. C., Jacobson, A. E., Burke, T. R., Jr., and Bajwa, B. S. (1983) Irreversible ligands with high selectivity toward μ or δ opiate receptors. *Science 220*, 314−316.
(25) Burke, T. R., Jr., Bajwa, B. S., Jacobson, A. E., Rice, K. C., Streaty, R. A., and Klee, W. A. (1984) Probes for narcotic receptor mediated phenomena. 7. Synthesis and pharmacological properties of irreversible ligands specific for μ or δ opiate receptors. *J. Med. Chem. 27*, 1570−1574.
(26) de Costa, B. D., Rothman, R. B., Bykov, V., Band, L., Pert, A., Jacobson, A. E., and Rice, K. C. (1990) Probes for narcotic receptor mediated phenomena. 17. Synthesis and evaluation of a series of *trans*-3,4-dichloro-*N*-methyl-*N*-[2-(1-pyrrolidinyl)cyclohexyl]-benzeneacetamide (U50,488) related isothiocyanate derivatives as opioid receptor affinity ligands. *J. Med. Chem. 33*, 1171−1176.
(27) Perret, P., Sarda, X., Wolff, M., Wu, T.-T., and Bushey, G. M. (1999) Interaction of non-competitive blockers within the γ-aminobutyric acid type A chloride channel using chemical reactive probes as chemical sensors for cysteine mutants. *J. Biol. Chem. 274*, 25350−25354.
(28) Levitsky, K., Boersma, M. D., Ciolli, C. J., and Belshaw, P. J. (2005) Exo-mechanism proximity-accelerated alkylations: Investigations of linkers, electrophiles and surface mutations in engineered cyclphilin-cyclosporin systems. *ChemBioChem 6*, 890−899.
(29) Krusemark, C. J., and Belshaw, P. J. (2007) Covalent labeling of fusion proteins in live cells via an engineered receptor-ligand pair. *Org Biomol. Chem. 5*, 2201−2204.
(30) Chen, Z., Jing, C., Gallagher, S. S., Sheetz, M. P., and Cornish, V. M. (2012) Second-generation covalent TMP-tag for live cell imaging. *J. Am. Chem. Soc. 134*, 13692−13699.
(31) Levy, R. H., Mattson, R., and Meldrum, B. (1995) *Antiepileptic Drugs.*, 4th ed., Raven Press, New York
(32) LeTiran, A., Stables, J. P., and Kohn, H. (2002) Design and evaluation of affinity labels of functionalized amino acid anticonvulsants. *J. Med. Chem. 45*, 4762−4773.
(33) Salome, C., Salome-Grosjean, E., Stables, J. P., and Kohn, H. (2010) Merging the structural motifs of functionalized amino acids and α-aminoamides: compounds with significant anticonvulsant activities. *J. Med. Chem. 53*, 3756−3771.
(34) Wang, Y., Wilson, S. M., Brittain, J. M., Ripsch, M. S., Salome, C., Park, K. D., White, F. A., Khanna, R., and Kohn, H. (2011) Merging structural motifs of functionalized amino acids and α-aminoamides results in novel anticonvulsant compounds with significant effects on slow and fast inactivation of voltage-gated sodium channels and in the treatment of neuropathic pain. *ACS Chem. Neurosci. 2*, 317−332.
(35) Salome, C., Salome-Grosjean, E., Park, K. D., Morieux, P., Swendiman, R., DeMarco, E., Stables, J. P., and Kohn, H. (2010) Synthesis and anticonvulsant activities of (*R*)-*N*-(4′-substituted)benzyl 2-acetamido-3-methoxypropionamides. *J. Med. Chem. 53*, 1288−1305.
(36) Anderson, G. W., Zimmerman, J. E., and Callahan, F. M. (1967) A reinvestigation of the mixed anhydride method of peptide synthesis. *J. Am. Chem. Soc. 89*, 5012−5017.
(37) Miyaura, N., and Suzuki, A. (1995) Palladium-catalyzed cross-coupling reactions of organoboron compounds. *Chem. Rev. 95*, 2457−2483.
(38) For a comparable procedure for resolving stereoisomers, see: Weisman, G. R. (1983) In *Asymmetric Synthesis-Analytical Methods* (Morrison, J. D., Ed.), Vol. *1*, pp 153−171, Academic Press, New York.
(39) Wang, Y., Brittain, J. M., Jarecki, B. W., Park, K. D., Wilson, S. M., Wang, B., Hale, R., Meroueh, S. O., Cummins, T. R., and Khanna, R. (2010) In silico docking and electrophysiological characterization of lacosamide binding sites on collapsin response mediator protein 2 (CRMP-2) identifies a pocket important in modulating sodium channel slow inactivation. *J. Biol. Chem. 285*, 25296−25307.
(40) King, A. M., Yang, X.-F., Wang, Y., Dustrude, E. T., Barbosa, C., Due, M. R., Piekarz, A. D., Wilson, S. M., White, F. A., Salome, C., Cummins, T. R., Khanna, R., and Kohn, H. (2012) Identification of the benyloxyphenyl pharmacophore: A structural unit that promotes sodium channel slow inactivation. *ACS Chem. Neurosci. 3*, 1037−1049.
(41) Kuo, C. C., and Bean, B. P. (1994) Slow binding of phenytoin to inactivated sodium channels in rat hippocampal neurons. *Mol. Pharmacol. 46*, 716−725.
(42) Rudy, B. (1978) Slow inactivation of the sodium conductance in squid giant axons. Pronase resistance. *J. Physiol. 283*, 1−21.
(43) Hodgkin, A. L., and Huxley, A. F. (1952) The dual effect of membrane potential on sodium conductance in the giant axon of Loligo. *J. Physiol. 116*, 497−506.
(44) Bean, B. P. (2007) The action potential in mammalian central neurons. *Nat. Rev. Neurosci. 8*, 451−465.
(45) Do, M. T., and Bean, B. P. (2003) Subthreshold sodium currents and pacemaking of subthalamic neurons: modulation by slow inactivation. *Neuron. 39*, 109−120.
(46) Vilin, Y. Y., and Ruben, P. C. (2001) Slow inactivation in voltage-gated sodium channels: molecular substrates and contributions to channelopathies. *Cell Biochem. Biophys. 35*, 171−190.
(47) Hinman, A., Chuang, H.-h., Bautista, D. M., and Julius, D. (2006) TRP channel activation by reversible covalent modification. *Proc. Natl. Acad. Sci. U.S.A. 103*, 19564−19568.
(48) Conaway, C. C., Krzeminski, J., Amin, S., and Chung, F.-L. (2001) Decomposition rates of isothiocyanate conjugates determine their activity as inhibitors of cytochrome P450 enzymes. *Chem. Res. Toxicol. 14*, 1170−1176.
(49) Macpherson, L. J., Dubin, A. E., Evans, M. J., Marr, F., Schultz, P. G., Cravatt, B. F., and Patapoutian, A. (2007) Noxious compounds activate TRPA1 ion channels through covalent modification of cysteines. *Nature 445*, 541−545.
(50) Vedantham, V., and Cannon, S. C. (1998) Slow-inactivation does not affect movement of the fast inactivation gate in voltage-gated Na^+ channels. *J. Gen. Physiol. 111*, 83−93.
(51) McCollum, I. J., Vilin, Y. Y., Spackman, E., Fujimoto, E., and Ruben, P. C. (2003) Negatively charged residues adjacent to IFM motif in DIII-DIV linker of $hNa_V1.4$ differentially affect slow inactivation. *FEBS Lett. 552*, 163−169.
(52) Chen, Y., Yu, F. H., Surmeier, J., Scheuer, T., and Catterall, W. A. (2006) Neuromodulation of Na^+ channel slow inactivation via cAMP-dependent protein kinase and protein kinase C. *Neuron 49*, 409−420.